The stabilizing effect of flow shear on $m/n=3/2$ magnetic island width in DIII-D

R. J. La Haye[1,a)] and R. J. Buttery[2]
[1]*General Atomics, P.O. Box 85608, San Diego, California 92186-5608, USA*
[2]*EURATOM/UKAEA Fusion Association, Culham Science Centre, Abingdon, Oxfordshire OX14 3DB, United Kingdom*

(Received 18 September 2008; accepted 12 January 2009; published online 20 February 2009)

It is found that flow shear has a stabilizing effect on $m/n=3/2$ neoclassical tearing mode islands through a more negative classical tearing stability index Δ' in the DIII-D [J. L. Luxon, Nucl. Fusion **42**, 614 (2002)] tokamak. The heating neutral beams are mixed between co- and counter-directions to vary the torque on the plasma and thus the plasma flow (rotation) and flow shear. This is done "shot to shot" in the presence of a saturated $m/n=3/2$ neoclassical tearing mode (NTM) while slowly raising the plasma beta up to the limit of the onset of an $m/n=2/1$ mode. A heuristic model for the stabilizing effect of flow shear on Δ' is shown to explain how flow shear acts to reduce NTM island size and obviate the effect of higher beta and concomitant destabilizing helically perturbed bootstrap current. © *2009 American Institute of Physics*. [DOI: 10.1063/1.3077673]

I. INTRODUCTION

Rotating tearing mode islands reduce energy confinement[1] and slow plasma rotation.[2] The reduction in energy confinement time is proportional to the full island width w, if the high confinement H-mode is retained. The expected drag on the plasma rotation is proportional to $w^3 - w^4$ depending on whether the drag is only on the plasma within the island (w^3) or global (w^4).[2] A too large island can cause mode locking to the wall, plasma rotation to stop, loss of H-mode, and disruption.[2,3] Neoclassical tearing modes (NTMs) are classically stable and sustained by a helically perturbed bootstrap current.[4] A NTM is initially destabilized when the "seed" from another magnetohydrodynamic (MHD) event exceeds the small island stabilizing effects. These effects become negligible at large island sizes. A saturated NTM island with $dw/dt \approx 0$ is expected to increase linearly in width with plasma beta proportional to the bootstrap current; this is provided that profiles remain nearly constant and the classical tearing stability index Δ' (Refs. 5–9) for the total current profile also remains unchanged.

A stable total current profile ($\Delta' < 0$) can be made more or less stable in the presence of flow and flow shear at the rational surface $q=m/n$, where m is the poloidal mode number and n is the toroidal mode number. Theoretical work has, so far, concentrated on the effect of equilibrium flow on the classical tearing stability. Several studies have predicted a stabilizing effect of sheared flow[10,11] and a strong effect on the island width;[12] although others have predicted only a modest[13] or even a destabilizing effect.[14] The latter, however, may be explained by a different choice of the relative signs of flow and magnetic shears. In another theoretical study, applying to DIII-D experimental observations, it was shown that a deformation of the magnetic island is caused by the viscous drag of a sheared flow.[15] The deformation was inferred experimentally from the radial profile of the electron cyclotron emission (ECE) at the $m/n=3/2$ island rotation frequency. The perturbed T_e phase, rather than the expected 180° jump in crossing the O-point, had a sheared phase jump attributed to the flow shear observed.

A recent experimental study on DIII-D showed that the onset beta for destabilizing $m/n=2/1$ NTMs decreased significantly as "co-injected" torque and rotation were reduced.[16] For the finite positive growth rate of an initially zero amplitude mode, flow and flow shear enter into the physics of Δ', and into both the threshold stabilizing effects and the seeding (coupling) from other MHD modes such as sawteeth and edge localized modes (ELMs).[4,16] The best correlation of the plasma beta at the onset of a $m/n=2/1$ NTM with the applied torque as found in Ref. 16 was with flow shear at $q=2$ as suggested by theoretical work on Δ' in Refs. 10–15. However, it was not possible to determine Δ' as a function of flow shear explicitly due to the complications of threshold and seeding effects on the onset.

In this paper, the effect of flow shear on existing "saturated" $m/n=3/2$ islands is presented. Here we evaluate modes (islands) with finite amplitude, and zero growth rate in contrast to the initially zero or small amplitude, finite positive growth rate for the $m/n=2/1$ mode studied previously. In Sec. II, the heuristic model for the normalized flow shear (NFS) is discussed in more detail than in Ref. 16. Section III has the experimental method used (as in Ref. 16 and using the same discharges) and the database of variation of flow and flow shear. Section IV has the main result of how the classical tearing index Δ' as a linear function of normalized flow shear (NFS) balances the helically perturbed bootstrap current allowing this assumed linear function to be determined. Conclusions and a discussion of new modeling and analytic theory in progress elsewhere are given in Sec. V.

a)Author to whom correspondence should be addressed. Electronic mail: lahaye@fusion.gat.com.

II. HEURISTIC MODEL FOR EFFECT OF FLOW SHEAR ON Δ'

The central idea which can be taken from previous theoretical studies is that flow shear can have a stabilizing effect on NTM islands through a more negative classical stability index Δ'. In the absence of flow shear, magnetic shear varies the field line pitch so that particles travel around the island center, the O-point. With $q=d\phi/d\theta$ and minor radius r, $q=m/n+(dq/dr)\delta r$ and $\delta\phi=[m/n+(dq/dr)\delta r]\delta\theta$, a field line stagnates on the O-point for $\delta r=0$ and rotates around it for $\delta r\neq 0$. This twists the field about the island, increases field line bending energy and makes tearing harder if the radial magnetic shear length $L_q=q/(dq/dr)$ is positive and the total current density radial shear length is negative.[7] We conjecture that flow shear can have a similar effect. The key element to consider is that flow shear can couple to the island through viscosity, locally perturbing both the particle trajectories and the field structure associated with the island.[15] This will change the degree of field line bending and energy required to drive the mode. Thus flow shear could have the same stabilizing effect as positive magnetic shear. The exact way in which these two types of shear will combine is difficult to predict without a more precisely calculated theory. However, the rotation shear will also act to distort the overall island shape (see figures discussed in next paragraph), and this effect might be more symmetric in terms of its effect on island magnetic structure (and so sign independent). The exact balance between these effects will depend on how the particle trajectory effect couples into island magnetic structure and drives, which needs more detailed calculation—we leave this to later more theoretical work, concentrating here on the implications in terms of how to measure and normalize quantities in the experimental effort. Thus the ratio of the flow shear with respect to the magnetic shear governs how significant the flow shear effect is. In addition, there is the issue of the relative sign. These factors can determine whether an initial island will decay or grow, ignoring neoclassical tearing effects (discussed later). The detailed directions for the usual co-neutral beam injection (co-NBI) in DIII-D are shown in Fig. 1. This has flow shear adding to magnetic shear (in the direction of the magnetic field) although the gradients are of opposite sign. Here only toroidal flow $V_{oz}(r)$ is assumed with the z the toroidal direction. Flow shear is the radial derivative of $\omega_{oz}=V_{oz}/R$ with R the major radius. Figure 2 shows what magnetic contours of an island with and without flow shear should look like and is adapted from Ref. 15. For the geometry of Fig. 1, the small arrows in Fig. 2(a) show how field lines go around the O-point (in the direction of the magnetic field) for positive magnetic shear. For Fig. 2(b), the large arrows show how negative co-flow shear (in the frame of zero flow at the O-point), i.e., in the rotating island rest frame add to the effect of the magnetic shear on particle trajectories in the direction of the magnetic field, and distort overall island shape. For normalization, we assume that, except in the very narrow tearing layer, resistive MHD is just ideal MHD field line bending propagating at the Alfvén velocity $V_A=B_{oz}/\sqrt{\mu_o n_e m_i}$ using the toroidal field for V_A and the local electron density n_e. Thus a characteristic

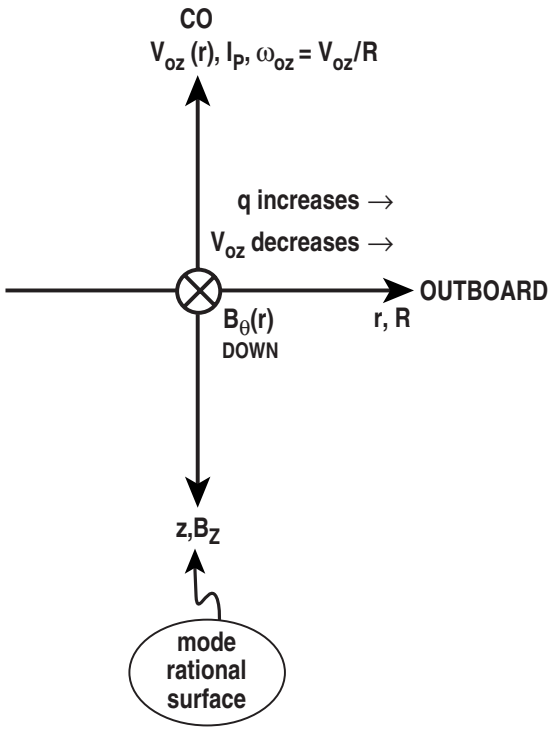

FIG. 1. Coordinates and directions for the magnetic field and flow in the usual co-NBI in DIII-D. Looking down on outboard midplane so z is in toroidal direction parallel to toroidal field B_{oz} but opposite to plasma current I_p and toroidal flow V_{oz} with $\omega_{oz}=V_{oz}/R$; q increases with minor radius r, V_{oz} decreases with r, poloidal field $B_{o\theta}$ is down in the θ direction.

time for normalizing flow shear is $\tau_A=R_o/V_A$, where R_o is the major radius of the flux surface axis. A characteristic magnetic shear length for normalizing flow shear is taken as the magnetic shear length L_s, which is approximately the projection of the radial magnetic shear length L_q in the toroidal direction; $L_s=qL_q/(r/R)$ for $L_q\equiv q/(dq/dr)$. L_s also arises in the parallel connection length along an island of full width w, $\lambda_\parallel=L_s/(k_\theta w/2)$ for $k_\theta\equiv m/r$.[4,17] Thus a working measure of significant flow shear is taken as the value of the product of the radial shear in toroidal flow times the projection of the radial magnetic shear length into the toroidal direction times the Alfvén time.

In this paper the positive NFS $-(d\omega_{oz}/dr)L_s\tau_A$ is experimentally shown to be a stabilizing quantity for co-NBI with positive magnetic shear. There is at present, no tractable analytic expression for Δ'(NFS) although such is under construction.[18] The simplest heuristic form for the effect of flow shear is here taken as, normalized by minor radius r_s,

$$\Delta' r_s = C_1 + C_2\left(-\frac{d\omega_{oz}}{dR}L_s\tau_A\right), \tag{1}$$

with ω_{oz} the toroidal angular rotation frequency, the gradient taken at the outboard midplane major radius R (which most diagnostics cover as will be discussed) and C_1 and C_2 constants to be fitted to experiment. Again $L_s\equiv qL_q/(r/R)$ and $\tau_A\equiv R_o\sqrt{\mu_o n_e m_i}/B_{oz}$. The form of Eq. (1) would give a sign reversal if the flow shear were to be reversed with respect to the magnetic shear. Such an effect seemed to be present in the $m/n=2/1$ onset scaling in Ref. 16, i.e., the critical beta

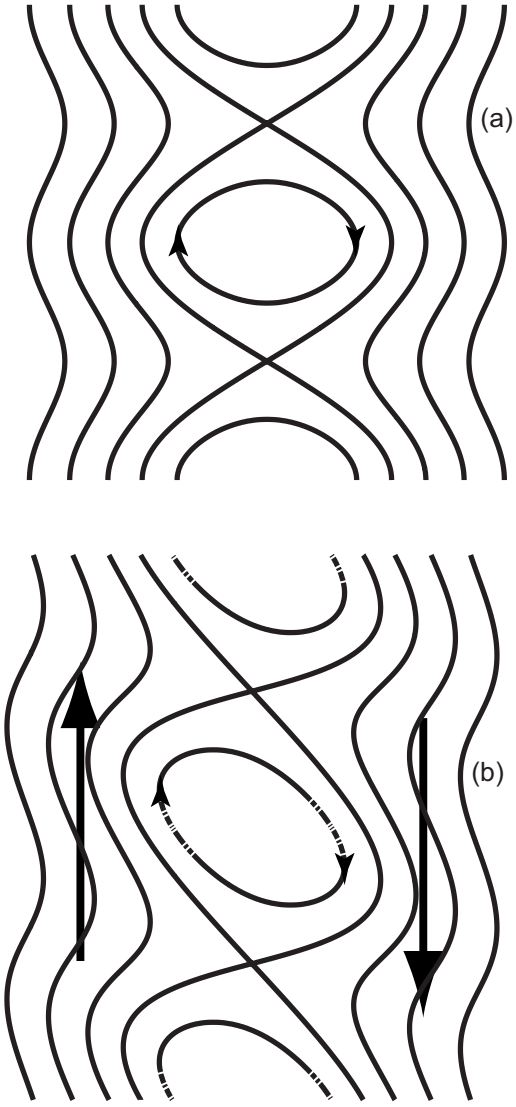

FIG. 2. (a) Magnetic flux contours of a magnetic island without flow shear. Arrows indicate direction traced by a puncture plot with positive magnetic shear and situation of Fig. 1. (b) An island deformed by flow shear. Arrows are for inboard co-flow greater than outboard co-flow in frame with zero flow at the rational surface. Sketch courtesy of P. A. Politzer.

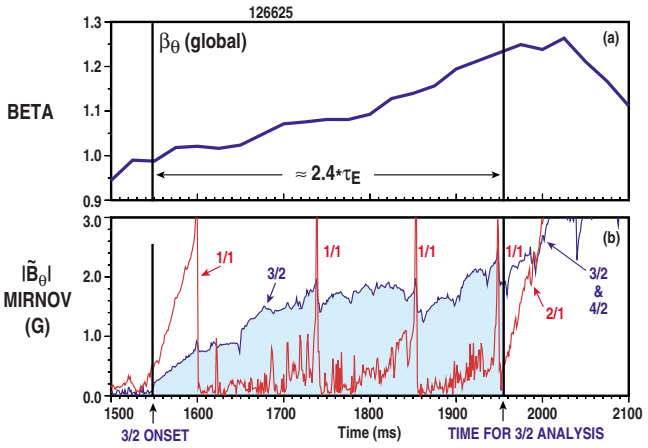

FIG. 3. (Color online) An example of a beta ramp under NBI feedback control, in a sawtoothing, ELMy *H*-mode with an $m/n=3/2$ NTM. (a) global β_θ noting the period between 3/2 onset and 2/1 onset is two to three energy confinement times. (b) Integrated Mirnov toroidal array amplitude for $n=1$ and $n=2$ modes. The shaded region is for the 3/2 NTM of interest here.

scales as $-\Delta' r_s$, which corresponds to Eq. (1) with a sign reversal if everything else were equal. Additional experiments in reversed I_p going further in the counter-rotation direction continue the trend to lower beta.[19] However the theoretical work does not suggest a sign dependence. In this case the bracket in Eq. (1) should use the absolute value. Adding the effects of magnetic shear and flow shear in quadrature would more properly use the square of the bracket. Note that the effect of flow shear in the theoretical work of Coelho and Lazzaro[11] did not depend on sign and appears to be closer to the form of Eq. (1) with the brackets squared. This will also be considered in the analysis of the experimental data.

The usual guess at $\Delta' r_s$ in previous experimental work for plasmas with strong co-flow is $-m$ [being between very stable $(-2m)$ and marginally stable (0) calculated with no shear flow].[3,7,20] With $C_2<0$, removing the usual flow shear would make $\Delta' r_s$ less negative (since $d\omega_{oz}/dR<0$), i.e., less classically stable. In principle, the value of C_2 might be related to the degree of viscosity of the plasma. One can anticipate that however complex the manner in which NFS enters into Δ', an expansion in small NFS would be to leading order of the form of Eq. (1). A nonlinear effect in Δ' (NFS) might occur as NFS approaches $O(1)$ but is not observed in the experimental fit as will be shown in Sec. IV.

III. EXPERIMENTAL METHOD AND DATABASE

This work involving the saturated $m/n=3/2$ island uses the same experimental method and discharges as utilized in Ref. 16 for the onset of an $m/n=2/1$ NTM but the analysis is done for the saturated 3/2 NTM just before the growth of the 2/1 mode. The plasma current $I_p=1.0$ MA is ramped up to flattop with toroidal field $B_{To}=-1.6$ T, minor radius $a=0.59$ m, major radius $R_o=1.73$ m, safety factor at the 95% flux surface $q_{95}=4.4$, lower single null divertor shape with elongation $\kappa=1.8$, and lower triangularity $\delta_L=0.70$. Periodic near axis $m/n=1/1$ sawteeth begin early in the discharge. NBI is applied to induce a prompt *L* to *H* transition, a short ELM free period, and then frequent ELMs (medium *n* peeling/ballooning ELMs). Plasma beta (ratio of volume averaged plasma pressure to magnetic field pressure) is then slowly raised under plasma control system feedback of the NBI. Early in this ramp an $m/n=3/2$ NTM is excited and after an initial fast growth, increases slowly in amplitude as beta rises. This last phase is shown in Fig. 3. From shot to shot, the NBI torque is varied from all co- (to I_p direction) beams, to a mix of co and counter through balanced injections, to the maximum available counter-injected beams.

The $m/n=3/2$ database here is a subset of the data in Ref. 16 in that only discharges with optimal $n=1$ error field correction are retained, and all have an $m/n=3/2$ mode slowly evolving during the slow beta ramp up to the onset of an $m/n=2/1$ NTM. Figure 4 shows that the $m/n=3/2$ Mirnov frequency scales well with twice (for $n=2$) the plasma toroidal rotation at $q=3/2$ from the charge exchange

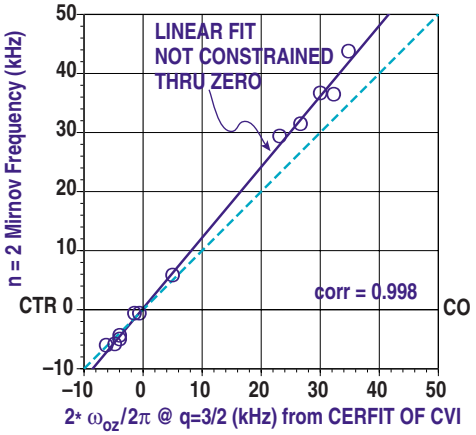

FIG. 4. (Color online) The $m/n=3/2$ Mirnov frequency versus twice the CER measured angular rotation ω_{oz} (divided by 2π) at $q=3/2$ for saturated 3/2 NTMs with rotation varied shot to shot by changing the co-counter NBI mix. Dashed line through zero for comparison.

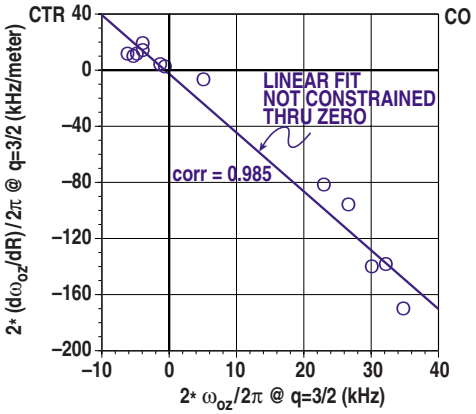

FIG. 6. (Color online) Flow shear $2(d\omega_{oz}/dR)/2\pi$ vs flow $2(\omega_{oz}/2\pi)$ at $q=3/2$ measured by CER at outboard midplane major radius. Fit yields a gradient scale length of 0.24 m.

recombination (CER) measure of CVI (carbon impurity) plasma rotation. A MHD equilibrium reconstruction is done for each discharge with the code EFIT constrained by the motional Stark effect (MSE) diagnostic of internal magnetic field pitch, shown in Fig. 5. Also shown are the locations of CER and of Thomson scattering. EFIT finds the $q=3/2$ surface location used for the CER measurement of rotation (Fig. 4).

Figure 6 gives the flow shear $d\omega_{oz}/dR$ at the $q=3/2$ outboard midplane major radius (see Fig. 5) versus flow ω_{oz} at $q=3/2$ measured by CER. The linear fit yields a consistent radial gradient scale length of 0.24 m. While flow can be transformed away, flow shear cannot. Also note that co-NBI has positive flow, decreasing with minor radius (negative flow shear); counter-NBI dominated has negative flow also decreasing in magnitude with minor radius but this is positive flow shear. The magnetic (L_q) and flow shear (L_ω) lengths are contrasted in Fig. 7. The extreme values of $L_\omega \equiv |\omega_{oz}|/(d\omega_{oz}/dR)$ in Fig. 7 come from nearly balanced rotation cases as can be inferred from Fig. 6. In fitting Δ', only the flow shear is used, not the scale length, as will be presented in Sec. IV.

Saturated NTM islands are sustained by a helically perturbed bootstrap current against a classically tearing stable total current density profile as described in Ref. 4 and many references therein. The simple form for the modified Rutherford equation (MRE) describing the growth of islands exceeding the small island threshold is

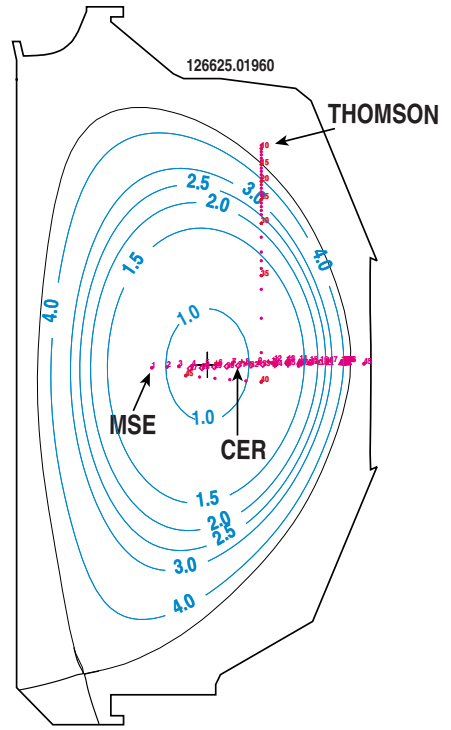

FIG. 5. (Color online) EFIT reconstruction of discharge of Fig. 2 at 3/2 analysis time. $q=1.0, 1.5, 2.0$, etc., surfaces noted, as well as locations of MSE, CER, and Thomson diagnostics. Note both the MSE and CER data overlap and span the radial profile from the magnetic axis to the plasma edge.

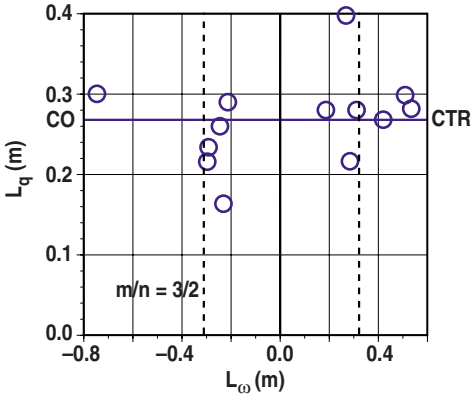

FIG. 7. (Color online) Radial magnetic shear length $L_q=q/(dq/dR)$ at outboard midplane major radius of $q=3/2$ (from EFIT) vs radial flow shear length $L_\omega=|\omega_{oz}|/(d\omega_{oz}/dR)$ from CER. Mean $L_q=0.27$ m, and mean $|L_\omega|=0.24$ m from Fig. 6. Mean $L_\omega=|\omega_{oz}|/(d\omega_{oz}/dR)$ for co and counter data are -0.31 and 0.32 m respectively.

$$\frac{\tau_R}{r_s}\frac{dw}{dt} = \Delta' r_s + \varepsilon^{1/2}\frac{L_q}{L_{pe}}\frac{r_s\beta_{\theta e}}{w}, \tag{2}$$

where τ_R is the resistive time equal to $1.22\ \mu_o\sigma\kappa r_s^2 T_e(\mathrm{eV})^{3/2}/Z_{\mathrm{eff}}$ with $\sigma=\sigma_o/f(\varepsilon)$ the Spitzer conductivity factor with finite aspect ratio trapping correction of $f(\varepsilon)$, κ is the elongation of the $q=m/n$ surface, T_e is the electron temperature at $q=m/n$, and Z_{eff} is the effective ion charge. We will be concerned with $\tau_R\dot{w}/r_s \approx 0$ in this paper. In addition, $\varepsilon=r_s/R_o$, $L_q=q/(dq/dR)$, $L_{pe}=-p_e/(dp_e/dR)$ noting the minus sign, and $\beta_{\theta e}=2\mu_o p_e/B_\theta^2$ is the local electron beta poloidal for electron pressure p_e. The form taken in Eq. (2) assumes the bootstrap current is dominated by and proportional to the electron pressure gradient. Thomson scattering (see Fig. 5) is used to measure p_e. EFIT locates the major radii of the $q=3/2$ surface at the midplane, R_{in} and R_{out}, with minor and major radii defined as $r_s \equiv (R_{\mathrm{out}}-R_{\mathrm{in}})/2$ and $R_o \equiv (R_{\mathrm{out}}+R_{\mathrm{in}})/2$; $B_\theta(R_{\mathrm{out}})$ is used in calculating $\beta_{\theta e}$, and the electron pressure profile from Thomson scattering is mapped to R_{out} for L_{pe}. The scale lengths in Eq. (2) are evaluated at the $q=3/2$ outboard midplane as is the NFS. The full outboard island width w comes from Mirnov loop analysis using EFIT as described in Ref. 19 and is corrected by a factor of 2/3 based on an ECE check of large islands at full toroidal field as also discussed in Ref. 20. The radial magnetic field perturbation at $q=3/2$ is $|\tilde{B}_r| \approx 0.5|\tilde{B}_\theta|_w(r_w/r_s)^{m+1}$, where a subscript w denotes the location of the Mirnov array ("wall") and $r_w=R_w-R_o$; full island width $w \approx C(8L_qR_o|\tilde{B}_r|/B_{T0})^{1/2}$, where $C=2/3$ is the ECE correction found for shaping, i.e., toroidicity. Thus $\Delta' r_s$ in Eq. (2) is a dimensionless classical tearing stability index and L_q/L_{pe} and r_s/w are dimensionless as are ε and $\beta_{\theta e}$.

One should note about this database that all discharges are sawteething so safety factor on axis is $q(0)\approx 1$ and all are well below the no wall ideal $n=1$ kink beta limit so that this is not an issue in Δ'.[9] The same shape and q_{95}, the same $q(0)\approx 1$, the same normalized minor radius $q=3/2$ location of $\rho_{32}=0.53\pm 0.01$ and midplane minor radius $r_s=0.35\pm 0.03$ m and major radius $R_0=1.73\pm 0.01$, and internal inductance $\ell_i=1.00\pm 0.03$ make for similar current density and q profiles and thus presumably $\Delta' r_s$ in the absence of flow shear effects.

IV. CLASSICAL TEARING INDEX Δ′ AND EXPERIMENTAL FLOW SHEAR

For saturated islands, the Eq. (2) is set to zero allowing the assumed negative $\Delta' r_s$ to be inferred from the measured quantities that make up the second term on the right hand side. This destabilizing helically perturbed bootstrap term is plotted in Fig. 8 against NFS at $q=3/2$ for each discharge. Note that both the y- and x-axis quantities in Fig. 8 are proportional to L_q. Thus y is essentially proportional to, in part, a pressure gradient, and x is proportional to, in part, a flow gradient. Evaluating gradients adds uncertainty of course, but is necessary, for this physics. The linear fit has a correlation coefficient of 0.80. All uncertainties given in this paper are to $\pm\sigma$, where σ is the standard deviation. For zero flow shear, $\Delta' r_s = C_1 = -1.9\pm 0.4$ is the zero flow shear classical tearing

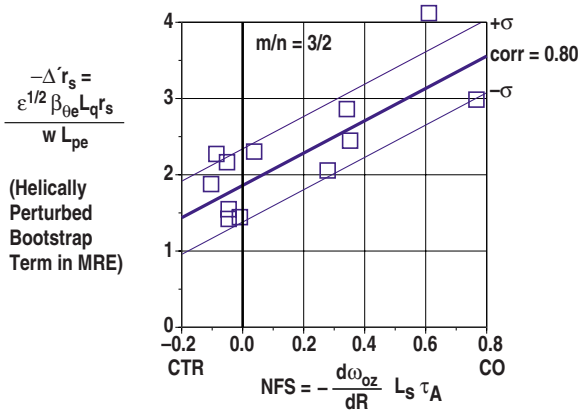

FIG. 8. (Color online) The value of $-\Delta' r_s$ inferred from the helically perturbed bootstrap term in the MRE plotted against NFS. Correlation of linear fit is 0.80 with $\sigma=0.48$ noted.

stability index. The linear term for the effect of NFS has a statistically significant multiplier of $C_2=-2.1\pm 1.4$. Thus an increase in tearing stability, i.e., twice as negative $\Delta' r_s$, occurs in going from zero flow shear to a value of NFS $=-(d\omega_{\mathrm{oz}}/dR)L_s\tau_A$ of $C_1/C_2 \approx 0.9$. Within the data, up to NFS of ≈ 0.8, there is no significant deviation from linearity. The all co-NBI case is fitted to have $\Delta' r_s \approx -3.6$, which is close to the approximation of $-m=-3$ used successfully to model mode evolutions with the MRE in previous experimental work with strong co-rotation; $C_1=-1.9$ and $C_2(-d\omega_{\mathrm{oz}}/dR)L_s\tau_A=-1.7$ is the added classical tearing stability due to the flow shear. An alternate linear fit to $|\mathrm{NFS}|$, not shown, is a close overlay to the linear fit to NFS of Fig. 8 and actually has a very slightly higher correlation coefficient of 0.82. A fit to a second order polynomial in NFS, also not shown, has almost zero coefficient in the NFS^2 term.

As Ref. 11 suggests a quadratic dependence (square of the NFS) without a linear term, the data of Fig. 8 is also fitted this way and shown in Fig. 9. The scales are kept the same for comparison. A factor of 2 increase in tearing stability occurs for a NFS of about 0.8 in this fit. The fit is not

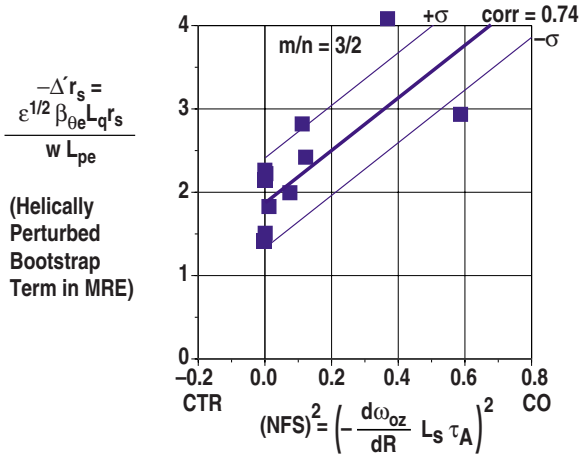

FIG. 9. (Color online) Same data as in Fig. 8 but the x-axis is now the square of the NFS; same scales as Fig. 8 for comparison. Correlation is 0.74 with $\sigma=0.54$ of the fit noted.

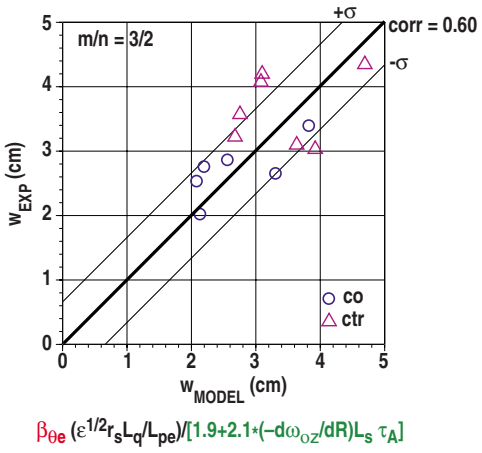

FIG. 10. (Color online) Experimental island widths vs fitted Δ' model Eq. (3) from linear fit shown in Fig. 8. The correlation is 0.60 with σ given. Open circles are co-dominated NBI cases and open triangles are counter-dominated or near-balanced cases. Red is destabilizing, black is neutral profile factor, and green is stabilizing with increased positive NFS.

quite as good as that of Fig. 8 with a smaller correlation (0.74 versus 0.80) and a larger sigma (0.54 versus 0.48); however it is evident that this cannot be ruled out with the existing data. Thus within this data, we cannot resolve a "sign effect" on reversing from co- to counter-rotation.

Note that in doing this experiment, more co-flow both increases the energy confinement time τ_E and improves $m/n=2/1$ tearing stability allowing going to higher beta before the 2/1 onset. This thus allows the increase of the plasma pressure and thus pressure gradient at $q=3/2$. A larger 3/2 island should result from the increased pressure gradient effect only. Balanced or small counter-rotation lowers τ_E, and the decreased 2/1 tearing stability and thus the lower beta reached should result in smaller islands, absent the flow shear effect. However, flow shear acts to reduce NTM island size and obviate the effect of higher beta. Figure 10 turns the linear NFS fit of Fig. 8 "around" to plot experimental island width versus the prediction of the $\Delta' r_s$ model fit,

$$w_{\mathrm{model}} = \beta_{\theta e}(\varepsilon^{1/2} r_s L_q / L_{pe})/[1.9 + 2.1(-d\omega_{\mathrm{oz}}/dR)L_s \tau_A]. \tag{3}$$

The co-dominated cases have a mean global β_θ of 1.3 ± 0.2; the counter- (or near-balanced) cases have 0.9 ± 0.1. Thus larger islands are expected for co-NBI if no flow shear effect; the opposite is observed due to negative flow shear and a more negative Δ'.

V. CONCLUSIONS

The stabilizing term $\Delta' r_s$ is inferred from its balancing the destabilizing helically perturbed bootstrap current term of the MRE, analyzed at a time when $dw/dt \approx 0$. By fitting the bootstrap current term (with all quantities from experimental measurements) to an assumed linear function of measured NFS, it is found that: (1) without flow shear, $\Delta' r_s$ is about -1.9 ± 0.4 in these plasmas with the same q_{95}, $q(0) \approx 1$, ℓ_i and ρ for $m/n=3/2$, (2) the effect of NFS is to make $\Delta' r_s$ twice as negative, i.e., stable, for NFS of about 0.9, i.e., $-d\omega_{\mathrm{oz}}/dRL_s\tau_A \approx 0.9$, and (3) the flow shear acts to reduce NTM island size and obviate the effect of higher beta. The choice of flow shear normalization by magnetic shear length $L_s = qL_q/(r_s/R)$ and Alfvén time $\tau_A = R_o\sqrt{\mu_o n_e m_i}/B_{\mathrm{oz}}$, suggested by theory, seems to work well in yielding the significant level of flow shear up to and including the highest value (≈ 0.8) achievable experimentally with all co-NBI. An alternate fit to the absolute value of the NFS is just as good and yields essentially the same quantitative result. While a linear dependence of Δ' on flow shear is a somewhat better fit to the data, a dependence on the square of the flow shear cannot be ruled out.

These results are motivating further theoretical modeling and analytic theory. This includes new work with the NEAR code,[12] new analytic theory in the "large m" approximation,[18] and new study of flow shear effects on islands with the NIMROD code.[21]

That flow shear has a stabilizing effect on NTM islands through a more negative classical stability index Δ' suggests that a large new tokamak such as ITER with larger inertia, little torque input, and expected low rotation may have relatively larger NTM islands than existing devices at similar beta and a lower beta threshold for onset. This makes electron cyclotron current drive stabilization of such islands even more critical than already anticipated.

ACKNOWLEDGMENTS

The authors acknowledge the many people of the DIII-D team who make running and diagnosing the discharges analyzed in this paper possible. They also gratefully acknowledge discussions of the theory of flow shear on tearing with Professor A. Sen of the IPR, Gujarat, India and Professor D. P. Brennan of the University of Tulsa.

This work was supported in part by the Engineering and Physical Sciences Research Council (U.K.), by the European Communities under the contract of Association between EURATOM and UKAEA, and by the U.S. Department of Energy under Grant No. DE-FC02-04ER54698. The views and opinions expressed herein do not necessarily reflect those of the European Commission.

[1] Z. Chang and J. D. Callen, Nucl. Fusion **30**, 219 (1990).
[2] F. F. Nave and J. C. Wesson, Nucl. Fusion **30**, 2575 (1990).
[3] R. J. La Haye, R. Prater, R. J. Buttery, N. Hayashi, A. Isayama, M. E. Maraschek, L. Urso, and H. Zohm, Nucl. Fusion **46**, 451 (2006).
[4] R. J. La Haye, Phys. Plasmas **13**, 055501 (2006).
[5] H. P. Furth, P. H. Rutherford, and H. Selberg, Phys. Fluids **16**, 1054 (1973).
[6] P. H. Rutherford, Phys. Fluids **16**, 1903 (1973).
[7] C. C. Hegna and J. D. Callen, Phys. Plasmas **1**, 2308 (1994).
[8] M. S. Chu, R. J. La Haye, M. E. Austin, L. L. Lao, E. A. Lazarus, A. Pletzer, C. Ren, E. J. Strait, T. S. Taylor, and F. L. Waelbroeck, Phys. Plasmas **9**, 4584 (2002).
[9] D. P. Brennan, R. J. La Haye, A. D. Turnbull, M. S. Chu, T. H. Jensen, L. L. Lao, T. C. Luce, P. A. Politzer, E. J. Strait, S. E. Kruger, and D. D. Schnack, Phys. Plasmas **10**, 1643 (2003).
[10] X. L. Chen and P. J. Morrison, Phys. Fluids B **2**, 495 (1990).
[11] R. Coelho and E. Lazzaro, Phys. Plasmas **14**, 012101 (2007).
[12] L. Ofman, P. J. Morrison, and R. S. Steinolfson, Phys. Fluids B **5**, 376 (1993).
[13] F. L. Waelbroeck, R. Fitzpatrick, and D. Grasso, Phys. Plasmas **14**, 022302 (2007).

[14]D. Chandra, A. Sen, P. Kaw, M. P. Bora, and S. Kruger, Nucl. Fusion **45**, 524 (2005).
[15]C. Ren, M. S. Chu, and J. D. Callen, Phys. Plasmas **6**, 1203 (1999).
[16]R. J. Buttery, R. J. La Haye, P. Gohil, G. L. Jackson, H. Reimerdes, and E. J. Strait, and the DIII-D Team, Phys., Plasmas **15**, 056115 (2008).
[17]R. Fitzpatrick, Phys. Plasmas **2**, 825 (1995).
[18]C. C. Hegna, Bull. Am. Phys. Soc. **52**, 129 (2007).
[19]R.J. Buttery, S. Gerhardt, A. Isayama, R. J. La Haye, E. J. Strait, D. P. Brennan, P. Buratti, D. Chandra, S. Coda, J. De Grassie, P. Gohil, M. Gryaznevich, J. Hobirk, C. Holcomb, D. F. Howell, G. Jackson, M. Maraschek, A. Polevoi, H. Reimerdes, D. Raju, S. Sabbagh, S. Saarelma, M. Schaffer, and A. Sen, Proceedings of the 22nd International Conference, Geneva, Switzerland, 2008 ["Multimachine extrapolation of NTM physics to ITER," Nucl. Fusion (submitted)].
[20]R. J. La Haye, R. J. Buttery, S. Guenter, G. T. A. Huysmans, M. Maraschek, and H. R. Wilson, Phys. Plasmas **7**, 3349 (2000).
[21]D. Brennan, personal communication (2008).